Some numerical results on the quasi-two-day wave excitation and propagation in the unstable summer middle atmosphere

E. Merzlyakov and Ch. Jacobi

Zusammenfassung

Mit Hilfe numerischer Simulationen wird gezeigt, dass manche Änderungen des klimatologischen Hintergrundwindfeldes zu instabilem mittleren Zonalwind in der mittleren Atmosphäre Sommerhemisphäre führen. Diese Instabilität treibt Oszillationen mit einer Periode um 2 Tage an, welche eine zonale Wellenzahl von s = 3 oder 4 aufweisen. Beobachtete Variationen des mittleren Windes stehen in Verbindung mit diesen numerisch gefundenen Schwingungen. Starke 2-Tage-Wellen wiederum sind instabil und können daher Wellen längerer Periodendauer und kleinerer Wellanzahl anregen. Dieser Effekt ist jedoch nur für sehr starke 2-Tage-Wellen signifikant. Effektiver ist ein Prozess, bei dem nichtlineare Wechselwirkung zwischen einer 10-14-Tage-Welle und der 2-Tage-Welle der zonalen Wellenzahl 4 eine neue quasi-2-Tage-Welle mit einer Periodendauer von 55-60 Stunden anregt. Diese Welle generiert sekundäre Wellen effektiver als die ursprüngliche 2-Tage-Wellen; die sekundären Wellen können beobachtet werden.

Summary

Basing on numerical calculations we have demonstrated that some changing of the climatological background atmosphere could lead to an unstable mean zonal wind distribution in the summer middle atmosphere. This instability forces oscillations propagating westward with a period of about 2 days and zonal wavenumbers s = 3 and/or 4. There are variations in the mean zonal wind distribution due to the excitation and transient propagation of these waves and numerical results correspond to features of these changes obtained in experimental studies. Strong 2-day waves in turn are unstable and can generate secondary waves with longer periods and lower zonal wavenumbers. This effect is significant only for very strong 2-day waves. It is shown that the 2-day wave with s=3 forced by non-linear interaction between 10-14 day planetary waves and the 2-day wave of zonal wave number 4 is unstable. This wave generates secondary waves of lower zonal wavenumbers more easily than the primary 2-day waves and these secondary waves may be observed.

1 Introduction

A strong quasi-two-day wave (QTDW) is a prominent feature of the atmosphere during solstice periods. This wave is a global planetary-scale oscillation, regularly observed by space based (e.g., Wu et al., 1996; Fritts et al., 1999; Lieberman, 1999) and ground based techniques (e.g., Muller, 1972; Kalchenko and Bulgakov, 1973; Jacobi et al., 2001). The meridional wind component of the wave is often greater than the zonal one at mid- and lower latitudes, although this is not always the case (Jacobi et al., 1997). Its amplitude may reach values up to 100m/s (Craig et al., 1980) during summer in the Southern hemisphere. Usually the QTDW in the Northern hemisphere has lower amplitudes. At Northern hemisphere mid-latitudes radar measurements give values of about 30 – 50 m/s for the meridional components and zonal wavenumbers s = 3-4 (Jacobi et al., 2001). From space-based observations these zonal wavenumbers are also inferred (Wu et al., 1996). For the Southern hemisphere the most prevailing 2-day wave has the zonal wavenumber s = 3.

The amplitude distributions of wind and temperature oscillations for the s = 3 wave are in a good agreement with those of the normal Rossby-gravity mode (Salby, 2001). The occurrence of this wave in the course of one year and its amplification during solstice periods may be explained as the normal mode behavior in the presence of a summer jet instability (Salby, 2001). However, this approach cannot explain the strong s = 4 wave with a period of 48h and lower. Plumb (1983) suggested baroclinic instability of the summer easterly jet as a source of the strong QTDW. Indeed global circulation models (Norton and Thuburn, 1999; Mayr et al., 2001) have demonstrated the occurrence of strong quasi-two-day waves with s = 3 and 4 due to baroclinic and barotropic instability of the summer mesospheric jet. Mayr et al. (2001) have shown that concomitant with these waves there is a whole spectrum of wind oscillations with periods close to periods of planetary waves. Ground-based and space-based measurements confirm the existence of 4-5 day waves and waves of longer periods during bursts of the QTDW.

However, Pfister (1985) showed that Newtonian cooling impedes an increase of the long-period waves. They do not reach significant amplitudes simultaneously with the QTDW. Possibly, there is another source of the long-period wind oscillations during the strong QTDW events. For example, Baines (1976) considered the stability of barotropic planetary waves and proved that the waves of full wavenumber (meridional index plus zonal wavenumber) greater than 2 are unstable. For a case of small amplitudes the unstable disturbances form a resonant triad with the primary wave. The increase depends on the amplitude of that wave, which is considered as the primary one (Gill, 1974). Phase profiles of the QTDW in the mesosphere are frequently observed being approximately barotropic. In this case such a mechanism may be a possible source of day-to-day wind variability. On the other hand it will be shown that this kind of instability can exist for a baroclinic case.

In this investigation we mainly consider the instability of strong 2-day waves under conditions that these waves being exited due to jet instability. It will be demonstrated that this source is not strong and can only create small amplitude waves (4-6 m/s for the strong QTDW) at low and high latitudes. However, for the very strong QTDW that sometimes is observed during Southern hemisphere summer the secondary waves may reach amplitudes of the order of 10 m/s. Another point considered in this study is a dependence of the QTDW parameters on the summer jet, in particular on its velocity. Also, the evolution of the background atmosphere due to interaction with the QTDW is taken into consideration. Salby et al. (2001) pointed out the possibility of the instability amplification by long-period waves usually observed in a winter hemisphere. This point is also considered with relation to the instability of the QTDW. In this work we used a simple 3-D nonlinear model designed for modeling of planetary wave propagation and interaction between waves in the atmosphere.

2 Data

In the left panels Fig.1 S-transform spectra (amplitudes in m/s) are shown for data obtained at Obninsk (55°N,37°E) during several years and Kharkov (50°N,37°E) in 1998 and 1999. Data for Kharkov were taken for a height of 88 km. Features of wind measurements at these sites can be found, for example, in Jacobi et al. (2001). The S-transform was suggested by Stockwell et al. (1996) and successfully applied, e.g., by Portnyagin et al. (1999). Periodogram analyses calculated for a time interval when 10-15 day wind oscillations were observed are also shown in Fig.1. As seen from the S-spectra a usual feature of the QTDW events is the occurrence of oscillations with periods of ~ 3-5 days and slightly more than 5 days. One may also see long-period oscillations with periods of 10-15 days and the 2-day wave decoupling on bursts. Apparent sources of the shorter-period oscillations are normal modes propagating from below and/or the summer jet instability obtained e.g., by Mayr et al. (2001). We propose another source, which links the appearance of the observed wind oscillations and explains their simultaneous existence.

Obninsk 1990

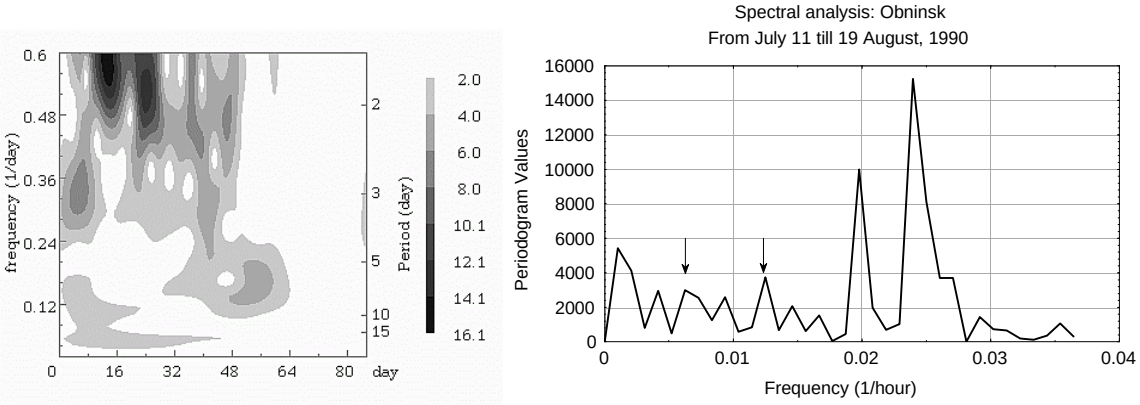

Obninsk 1991

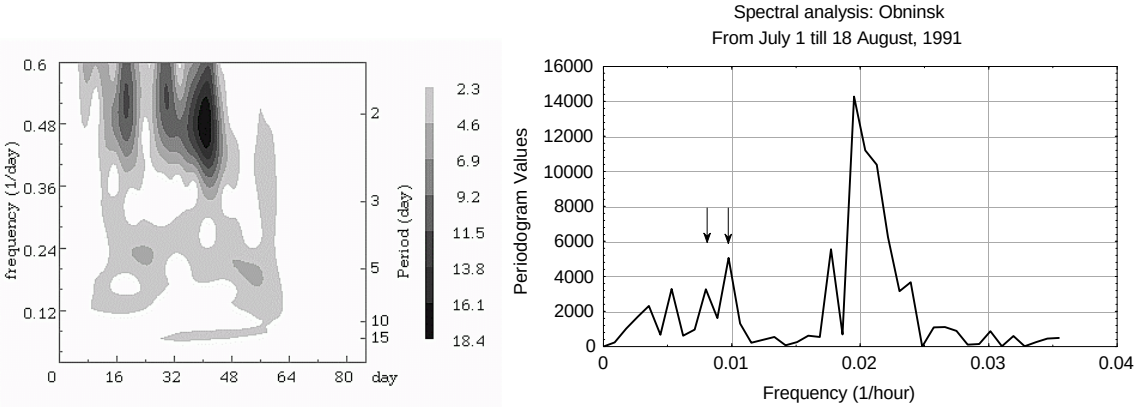

Kharkov 1998

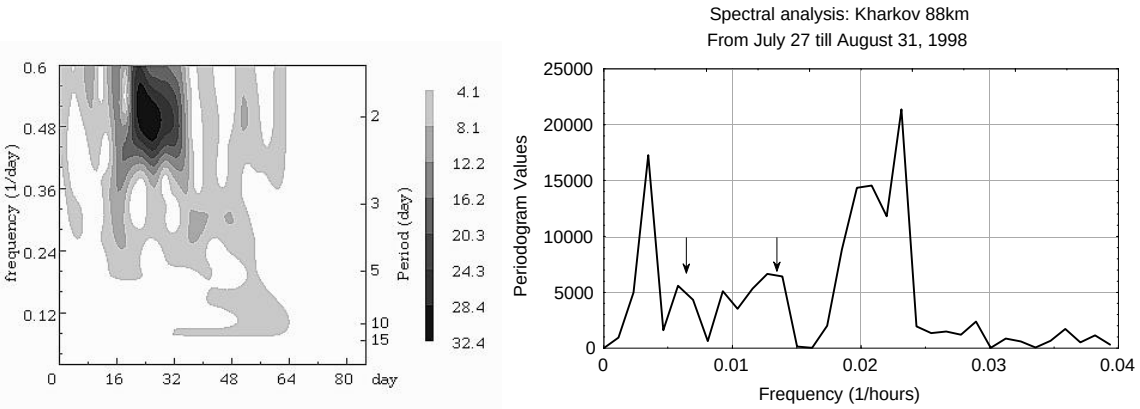

Kharkov 1999

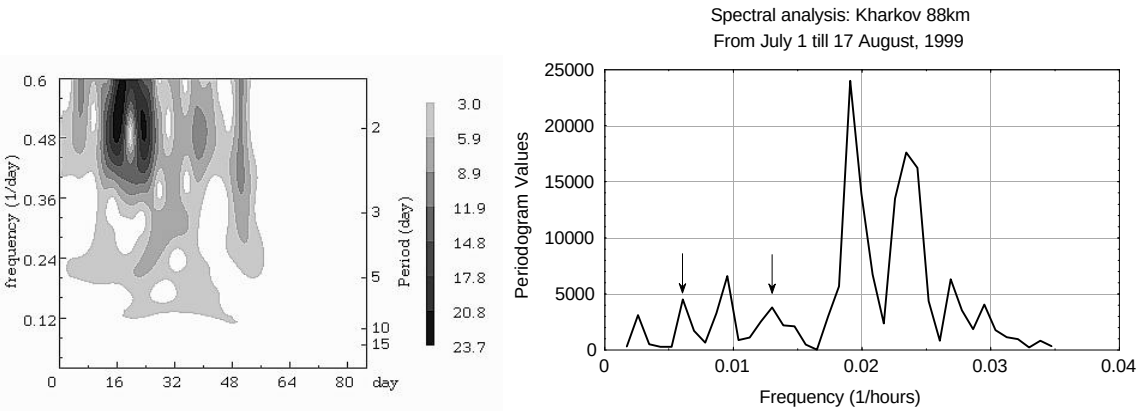

Figure 1: *S-transform spectra of zonal wind variations from July 1 to August 31 (left panels). Amplitudes (m/s) are shown by scales of grey. Periodograms (right panels) of zonal wind variations calculated for some subintervals of the measurements are also shown.*

Without measurements at other heights it is impossible to define whether both 2-day wave peaks are excited due to jet instability or one of them is a primary peak. However, for summers 1991 and 1998 one of the 2-day peaks looks like a secondary one, i.e. like a result of non-linear interaction between the primary oscillation and a planetary wave.

Arrows in the periodograms point out peaks whose sums of frequencies equal the frequency of the 2-day oscillations. Hence Figure 1 demonstrates the possible existence of peaks, corresponding to resonance triads.

Presently, there is no experimental measurement study, which considers common features of mean zonal wind changes before, during and after the QTDW burst. Nevertheless, there are several case studies showing a definite decrease of the mean zonal wind during the QTDW at lower and middle latitudes at heights of about 70-90 km (e.g., Plumb et al., 1987; Lieberman, 1999; Jacobi et al. 2001 ; Gurubaran et al., 2001). After this decrease there is recovering of the zonal wind (Gurubaran et al., 2001; Jacobi et al., 2001). A zonal wind increase at the beginning of the QTDW at some latitudes can be noted, too. This was also pointed out by Fritts et al.(1999) and is visible from results by Jacobi et al. (2001). We will refer to these results comparing them with simulated changes of mean zonal wind due to the QTDW.

3 Simulation approach

In our simulations, the unstable background state is achieved by introducing an additional mean zonal forcing of the form $F = 1/\rho\ \partial/\partial z(\rho F)$ into the momentum equation for the mean zonal wind. Three cases are considered. For the fist one F is a Gaussian hat on latitude and height. Other variants use a half of a sinusoid on latitude and the hat on height. To obtain a growing wave it is also necessary to introduce some noise into the model. This is realized as several waves of small variable amplitudes. These waves are exited near a height of 56 km with zonal wavenumbers from 1 to 5 by a thermal source localized on height in the summer hemisphere. Perturbations of wind velocities are of the order of few tens of sm/s due to this noise at heights of 60-90 km. The obtained results have a weak dependence on the respective realization of the noise. It is supposed that the noise is first of all a natural stochastic noise in the earth atmosphere. An additional source can be provided by weak 2-day oscillations from the lower part of the atmosphere and by nonlinear interaction between planetary waves (for example, 4- and 5-day waves).

Model runs without the noise were used for the input estimation of our artificial redistribution of the background atmosphere. The mean zonal forcing leads to a decrease of the negative meridional gradient of the potential vorticity, a decrease of the mean zonal wind, and the jet core is shifted towards the equator. Such a behavior of the jet does not contradict observations by Limpasuvan et al. (2000). The model is described in the Appendix.

4 Results

In the first model experiment a position and strength of the zonal forcing are tuned to give the instability near 30° latitude at 60 km height. This corresponds to results by Norton and Thuburn (1999). Wu et al. (1996) observed the main QTDW activity at latitudes of 20-30°S. Figure 2 presents results, obtained for this case. In the top left panel the reference mean zonal wind distribution without additional forcing ($F = 0$) is presented. The other rows present results with increased zonal forcing. In the right panels the corresponding distributions of the QTDW meridional wind amplitudes are presented. For this case the instability was obtained only the s = 3 wave. The amplitude of the wave is presented for time of wave maximum, while the mean zonal wind distributions are given for the time, when the minimum value of mean zonal wind is achieved. Periods are pointed for the strongest spectral components. Every spectral peak has a finite width due to amplitude changing as a result of instability. The

increase of the easterly jet corresponds to a decrease of the negative latitudinal gradient of the potential vorticity.

In the following we discuss the case with largest wave amplitudes (lowermost panels in Figure 2. The amplitude of the meridional wind component peaks at about 80 m/s and the temperature peak amplitude is about 10 K. The period of the 2-day wave is about 51.5 h. In Figure 3a) the mean zonal wind is shown at 90 km for different latitudes. The meridional wind component of the 2-day wave is shown for latitude 60° and with a half of amplitude.

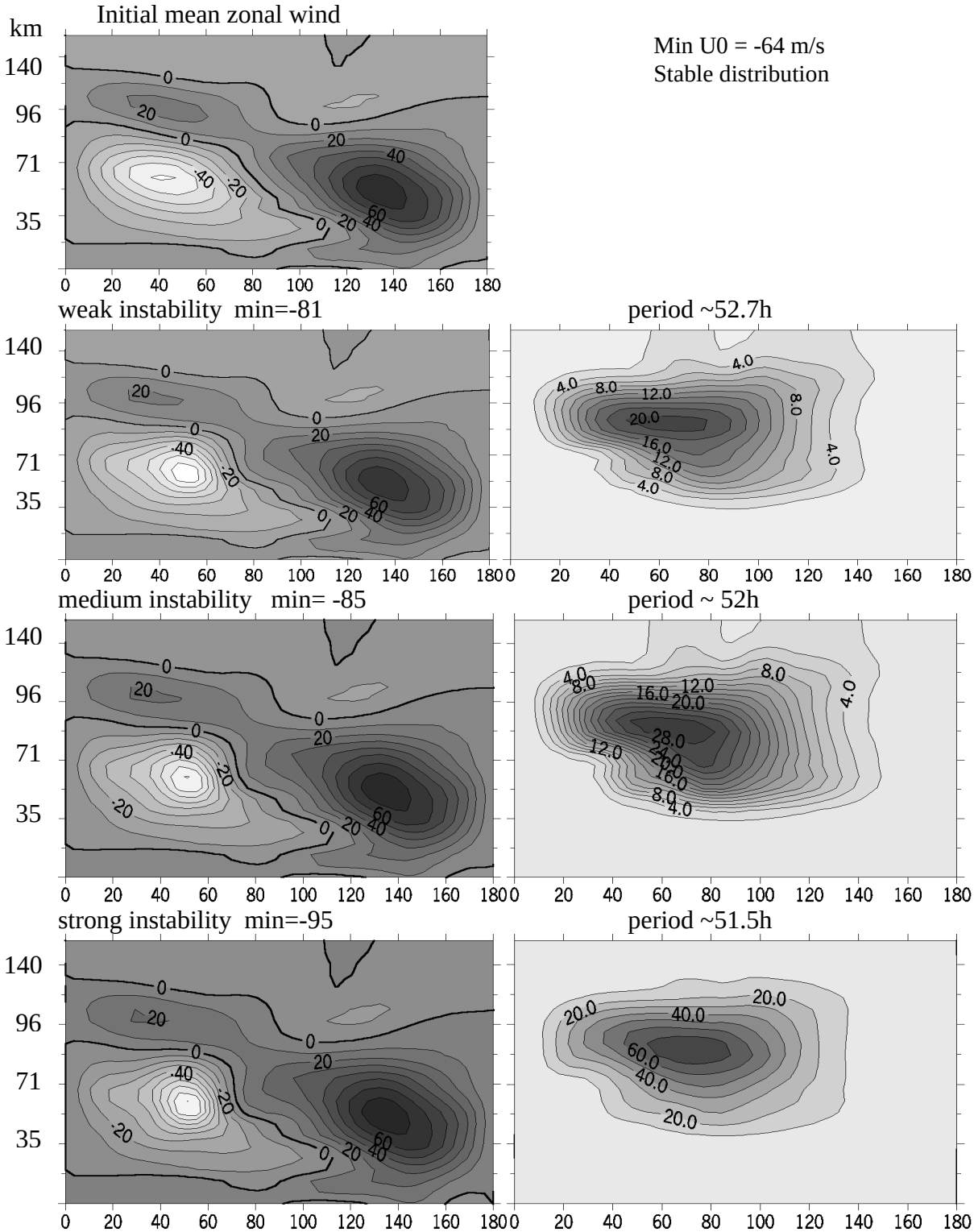

Figure 2: *Dependence of the amplitude (in m/s) of the 2-day wave (right panels) on the velocity of the easterly jet (left panels, values given in m/s). Axis labels are approximate altitude and colatitude.*

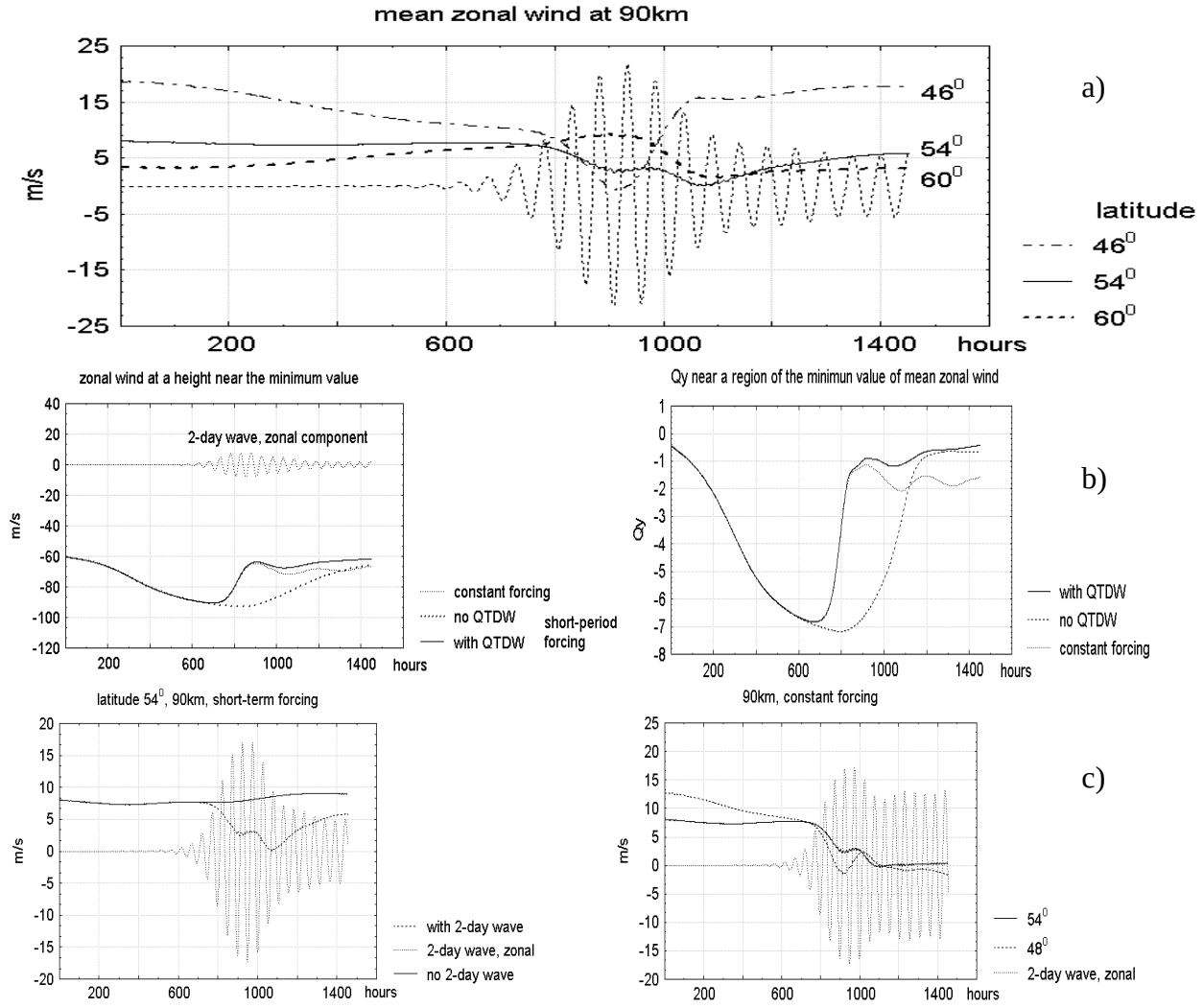

Figure 3*: a) variations of mean zonal wind at different latitudes at 90 km, and the meridional QTDW wind (divided by a factor of 2), b) zonal wind and QTDW amplitude at the height and latitude of the maximum easterly jet (left panel) and latitudinal gradient of the potential vorticity (right panel), c)left panel: mean wind at 54°N and 90 km with and without short-term forcing of QTDW, right panel: mean winds with constant forcing. The QTDW is also added.*

The zonal wind behavior is a result of both artificial wind changing to obtain the instability and the QTDW. It is possible to check how this artificial approach corresponds to experimental data. One can see a tendency that this course changes their character from high-latitudes to lower ones. Fritts et al. (1999) have considered changes of the mean zonal winds during the QTDW for different latitudes in the Southern hemisphere in summer of 1994. The tendency obtained in the model run is similar to that observed by Fritts at al. (1999), but it is valid for higher latitudes than in the experiments. Taking into account that the QTDW of winter 1994 were concentrated near the equator, it may be concluded that the numerical model reproduces some features of the QTDW in the Southern hemisphere summer.

The variation of the mean zonal wind and of the latitudinal gradient of the potential vorticity (Qy) near the region of the easterly zonal wind maximum are shown in Fig. 3b). A case called 'no QTDW' is obtained by removing noise with s = 3 from the model. Units of Qy are $1.14 \cdot 10^{-11} s^{-1} m^{-1}$. Fig. 3a,b) show that during the 2-day wave exiting the mean zonal wind and the meridional gradient of potential vorticity tend to values close to those for unforced case. This is the case even for constant forcing. These significant changes mean that the 2-day wave may influence the climatological wind distribution.

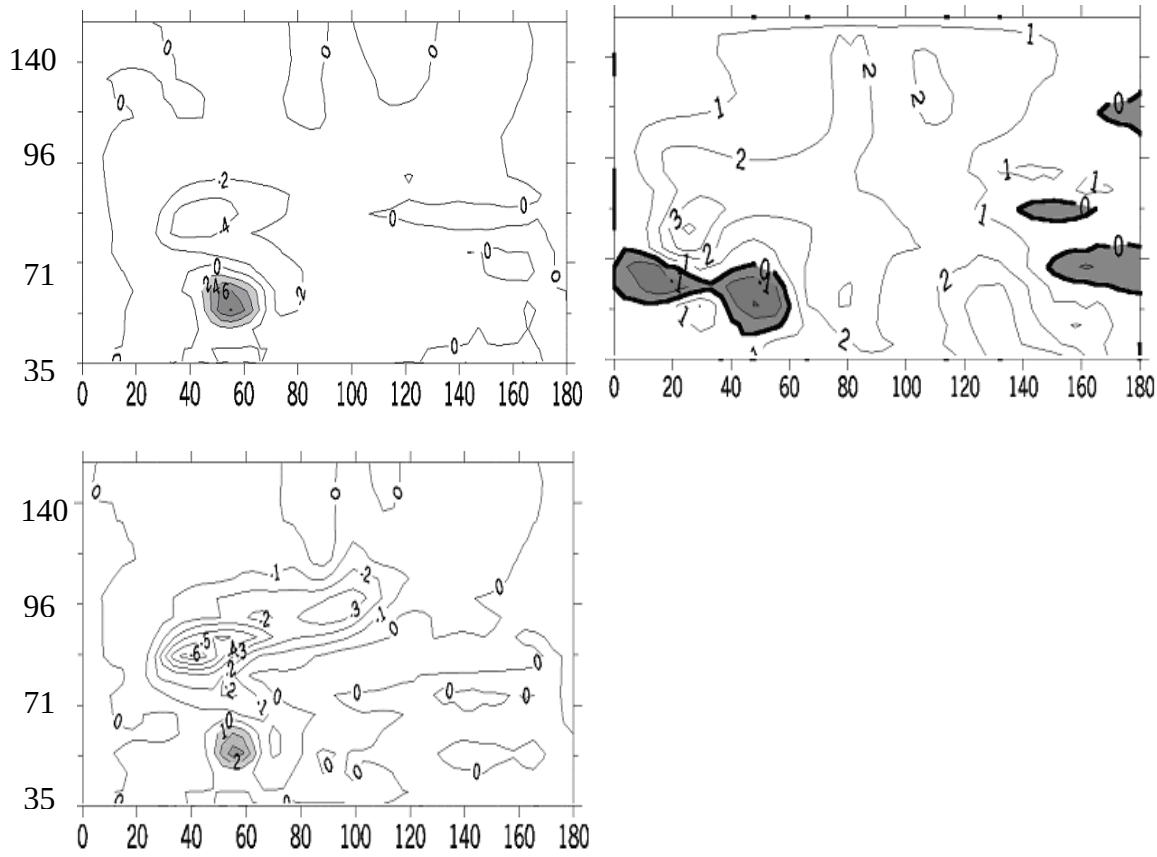

Figure 4: *EP flux divergence div **F** per unit mass, given in 2 m/s/day (upper left panel) and the latitudinal gradient of the potential vorticity (upper right panel). In the lower panel div **F** for a case of constant forcing near a time when the QTDW amplitudes are approximately constant. Axis labels are approximate altitude and colatitude.*

Figure 3c) shows a comparison between constant and short-term zonal mean forcing. For each case there is a burst of the wave activity and increasing of easterly winds due to the QTDW after generation of these waves.

In Figure 4 the divergence div **F** of Eliassen-Palm (E-P) flux and the latitudinal gradient of potential vorticity are presented for a case of short-term forcing (top). Here div **F** is presented in 2 m/s/day. These distributions are calculated for the time near the middle of the time interval of the QTDW increasing. At this time the region with strong latitudinal gradient of potential vorticity has practically disappeared. The response of the background atmosphere on the QTDW may be connected with two main processes. The first one is the excitation of the QTDW at some heights and latitudes where we observe div **F** > 0 and increase of westerly winds. The second process takes place above the excitation region, where div **F** < 0 and increase of easterly winds is observed. The latter feature is regularly noted in results based on radar wind measurements (e.g., Plumb et al., 1987; Gurubaran et al., 2001; Jacobi et al., 2001). However an existence of some increase of westerly winds near the mesopause was possibly noted only by Fritts et al. (1999). This increase takes place before the QTDW reaches its maximum amplitude and we connect it with the first process.

The lowermost panel in Fig. 4 shows div **F** for a case of constant forcing near the time, when amplitudes of the QTDW are approximately constant. The region of the positive E-P flux is dark and shows a wave activity production. This corresponds to Fig. 3b) where the mean zonal wind velocity is significantly larger than that one for the case without the QTDW. The phase velocity near the region of divergent E-P flux is about 67 m/s, and the wave amplitude of the meridional component is about 30 m/s. Their ratio is about 0.5, which means

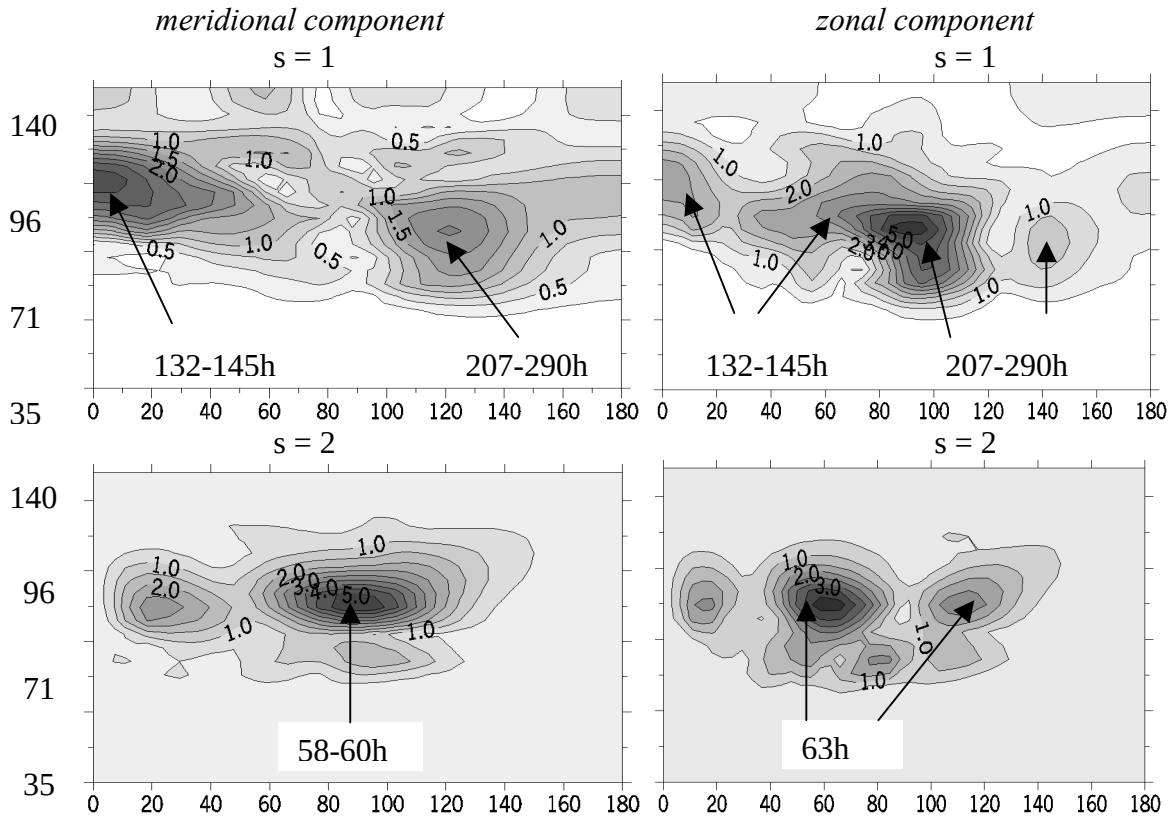

Figure 5: *Amplitudes (m/s) of secondary waves for zonal wave numbers 1 and 2, for the case of strong instability in the lowermost panel of Figure 2. Periods (hours) are pointed at by arrows. Axis labels are approximate altitude and colatitude.*

significant non-linearity that results in the exiting of secondary waves and energy flux to these waves. Dissipative terms are about an order of magnitude smaller than the non-linear ones. Thus, for the case with constant forcing we observe nearly constant wave amplitudes but the wave is exited permanently and E-P is divergent. Possibly, this divergence is balanced by terms that appear due to non-linearity.

Strong perturbations of zonal wavenumbers 1 and 2 appear during the 2-day wave exiting, too. They do not appear if the 2-day wave is absent. To check this, a special model run was carried out with conditions for the instability but without noise with s = 3. The increase of perturbations with s = 1,2 takes place only at the time of the 2-day wave exciting.

These secondary waves for the case of largest amplitudes from Figure 1 are shown in Figure 5. Frequencies of these waves and their zonal wavenumbers tend to create resonance triads with the 2-day wave. Hence, these waves possibly correspond to the 2-day wave instability. The distributions are shown for different periods which values are pointed in the figure. The oscillation with s = 1 and period of 132-145 h does not have its counterpart, but for the more strong instability (not shown) the counterpart was well observed. Possibly there is an interaction between oscillations more complex than those building of resonant triads or this oscillation is forced when the 2-day wave significantly increases. For the latter case it is difficult to indicate a periodic oscillation. The growth of the secondary waves is significantly dependent on the amplitude of the primary 2-day wave. For the case with the maximum jet value of -85 m/s the amplitudes of secondary waves are 2-3 times smaller than for the case of strong instability. This value approximately equals to the ratio of the amplitudes of the 2-day waves for these cases. In the case when the amplitude of the meridional wind component is about 111 m/s (not shown, this case corresponds the jet maximum of –110 m/s), the

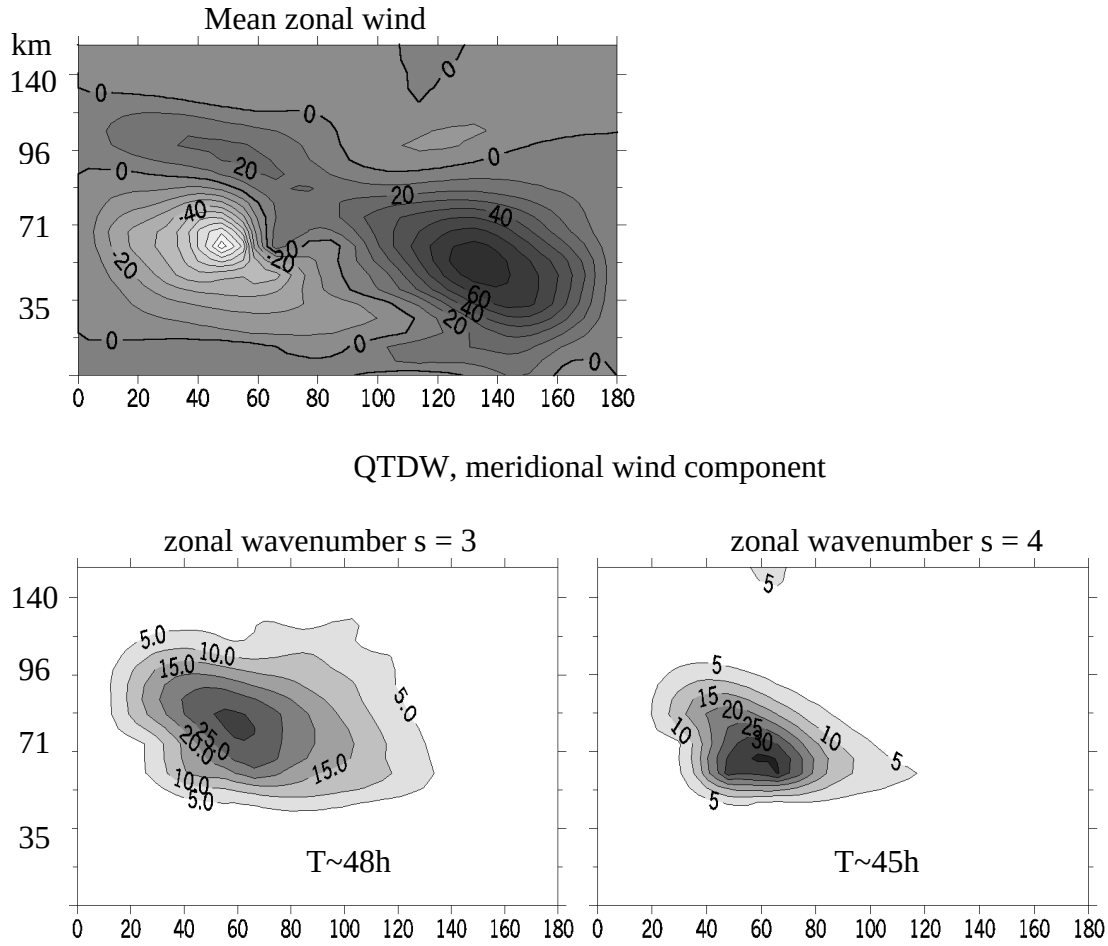

Figure 6: *Distributions of mean zonal wind and meridional wind amplitudes of waves 3 and 4. Amplitudes are given in m/s. Axis labels are approximate altitude and colatitude.*

secondary waves have amplitudes about four times larger at high-latitudes and nearly the same ones as for the presented cases at low latitudes.

The results for the second model experiment are presented in Figures 6-8. The unstable zonal wind distribution and the amplitudes of the meridional wind components for the s = 3 and 4 waves are shown in Figure 6. These waves reach their maximum at different times and are presented here near the time of maximum. The maximum value of the mean zonal easterly wind is –107 m/s. This value is necessary to obtain a stronger gradient of the potential vorticity than that for the first experiment. In turn, this Qy gradient is necessary to obtain strong waves of zonal wavenumber 4. As is visible, the s = 4 wave does not propagate far from its source. This result is similar to that obtained by Mayr et al. (2001). It means that at mid-latitudes one may observe both waves, while at lower latitudes the s = 3 wave would be predominant, if there is no s = 4 wave source located higher than in our simulation. At present it is difficult to check this conclusion from experimental results. Variations of mean zonal winds at different latitudes at about 90 km are shown in the right panel of Figure 7. As with the first experiment these curves are due to the artificial mean zonal wind forcing and the QTDW. For all latitudes there is an increase of easterly winds after the appearance of the QTDW and at latitude 36° there is an increase of westerly winds, too. This increase exists also for latitudes higher than 54° (not shown) and can be revealed in experimental data (see section 2).

In Figure 8 secondary waves are presented for this considered case. Their frequencies and zonal wavenumbers again create resonance triads with wave number s = 3. These waves disappear rather quickly due to dispersion (see Figure 7), which takes place at the moment of

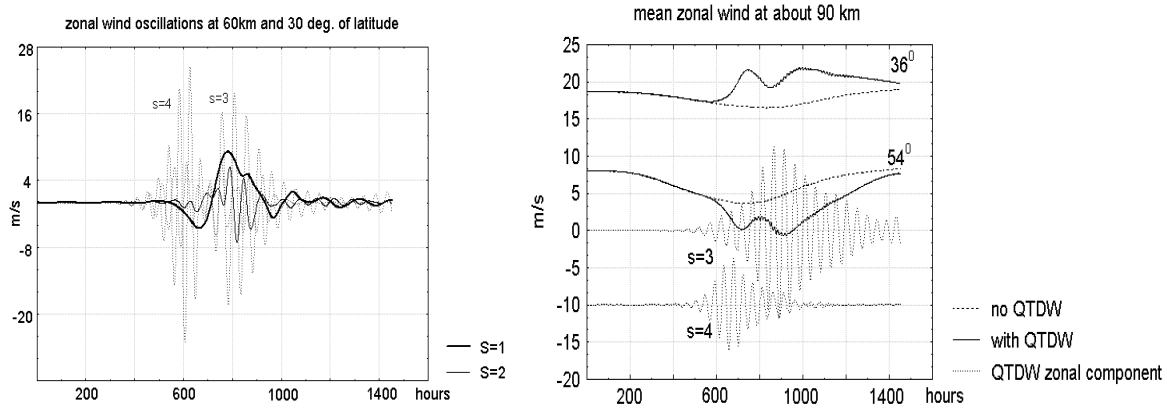

Figure 7: *Zonal wind oscillations for different zonal wavenumbers near the region of jet instability (left panel). Mean zonal wind changing due to excitation and propagation of the 2-day wave (right panel).*

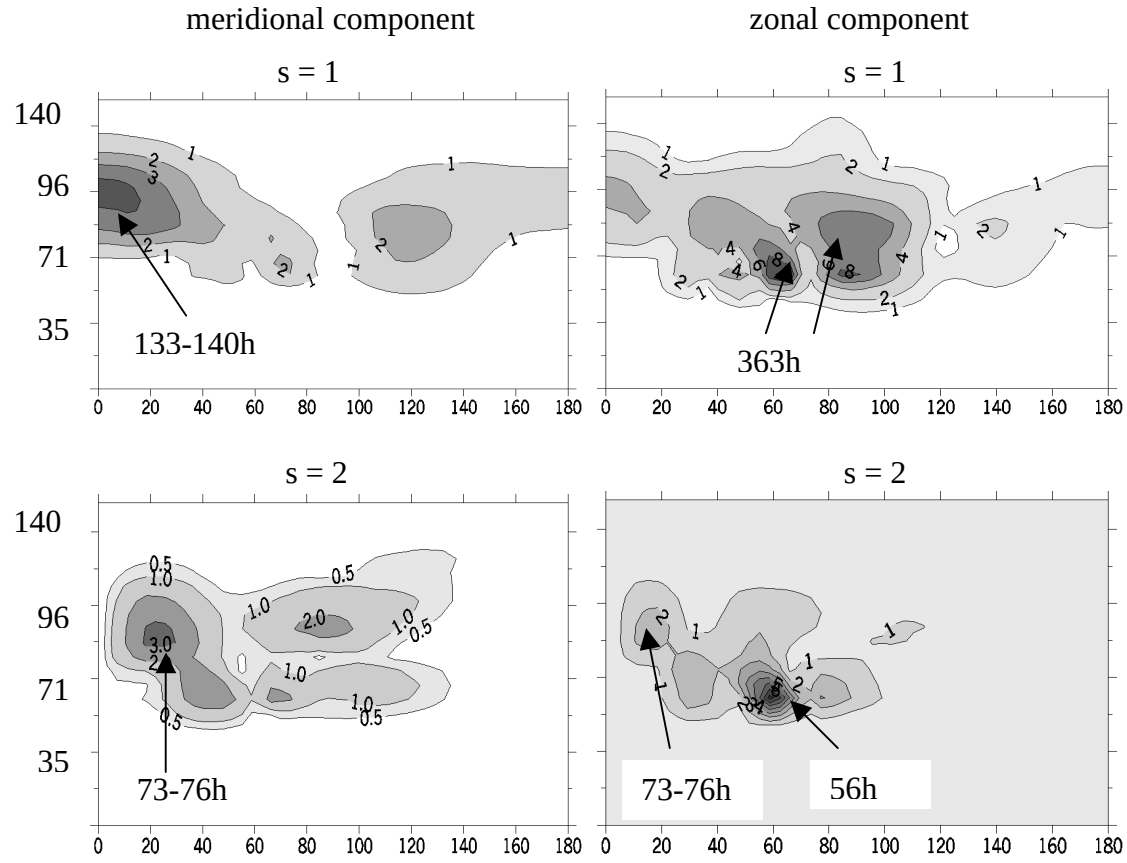

Figure 8: *Amplitude distributions (m/s) of secondary waves for zonal wavenumbers 1 and 2. Axis labels are approximate altitude and colatitude.*

exiting of the s = 3 wave. Significant secondary waves with a participation of the s = 4 wave are not observed.

The third variant of forcing is similar to that for the second experiment, but it is placed 5 km higher. The maximum velocity of the summer jet before the instability is –111 m/s. For this case the s = 3 wave is weak and the s = 4 wave is the main 2-day wave. Long-period waves with periods of 12-14 days are observed. Their role is of two kinds for the considered numerical experiment. The first one is the amplification of the instability and consequently of the 2-day wave. The second one is to transfer energy from s = 4 to the s = 3 wave. The latter wave

is found to be unstable and as a result one may observe two other waves with zonal wave number s = 2 and s = 1. This is demonstrated in Figure 9 for middle latitudes and may be compared to observational results in Figure 1.

5 Discussion

A possible mechanism, which may explain, why the secondary waves appear with large amplitudes of the 2-day wave and why their amplitudes strongly depend on the amplitude of this wave, may be obtained from a consideration of the non-linear wave interaction in the limit of small amplitudes. An additional condition for this simplified consideration is the absence of critical lines. At least for our first model experiment we may consider that the 2-day wave is mainly located far from its critical lines. It is known that plane Rossby waves of both small and large amplitude are unstable, and that for small amplitudes the unstable disturbances forms a resonant triad with the primary wave. The increment depends on the amplitude of that wave, which is considered as a primary (Gill, 1974). Let us consider a one-dimensional case of quasi-geostrophic flow on a mid-latitude beta-plane. There is no any dissipation. The notation are the same as in Plumb (1983). The basic state potential vorticity gradient is

$$\frac{\partial \bar{q}}{\partial y} = \hat{a} - \frac{f^2}{\tilde{n}} \frac{d}{dz}\left(\frac{\tilde{n}}{N^2}\frac{d\bar{u}}{dz}\right), \tag{1}$$

where $\bar{u} = \bar{u}(z)$ is the mean zonal flow, and the buoyancy frequency is $N=N(z)$. The main governing equations are the continuity equation and the definition of the quasigeostrophic potential vorticity (see, e.g., Andrews et al., 1987, p.122):

$$\frac{\partial q}{\partial t} + u\frac{\partial q}{\partial x} + v\frac{\partial q}{\partial y} = 0, \tag{2}$$

$$q = f + by + y_{xx} + y_{yy} + \frac{f^2}{r}\frac{\partial}{\partial z}\left(\frac{r}{N^2}\frac{\partial y}{\partial z}\right), \tag{3}$$

while $u=-y_y$ and $v=y_x$. y is the stream function and q is the potential vorticity. Following Davis and Acrivos (1967), we consider waves of small but finite amplitude. In the first order we get a linear equation and looking for solutions of the form

$$y_a = A_a(t)\, R_a(z) \exp(i\omega_\alpha t + ik_\alpha x + in_\alpha y), \tag{4}$$

where $A_a(t)$ is a slowly varied amplitude, t is a 'slow' time. For $R_a(z)$ we obtain the following equations:

$$(\omega_\alpha + \bar{u}\, k_\alpha)\left[-(k_\alpha^2 + n_\alpha^2)R_a + \frac{f^2}{r}\frac{d}{dz}\left(\frac{r}{N^2}\frac{\partial R_a}{\partial z}\right)\right] + \bar{q}_y R_a k_\alpha = 0, \tag{5}$$

and

$$q_a = \frac{-k_a}{w_a + \bar{u}k_a} y_a \bar{q}_y \ . \tag{6}$$

For the second order on amplitude we take into account non-linear terms. We are interested in the case of three waves which are coupled through a resonant interaction, that is

$$\mathbf{k_á} + \mathbf{k_â} = \mathbf{k_2} \quad \text{and} \quad \omega_\alpha + \omega_\beta = \omega_2, \tag{7}$$

where $\mathbf{k_a}=(k_\alpha, n_\alpha)$. The equation for a mode with zonal wavenumber k_2 is following:

$$i(\omega_2+\bar{u}\,k_2)[-(k_2^2+n_2^2)R_2A_2+\frac{f^2}{r}\frac{d}{dz}(\frac{r}{N^2}\frac{\partial R_a}{\partial z})A_2] + i\bar{q}_y R_2 A_2 k_2 + \frac{\partial A_2}{\partial t}R_2 + \sum_{\mathbf{k_a}+\mathbf{k_b}=\mathbf{k_2}}\left[\frac{k_b(k_a n_b - k_b n_a)}{\omega_b+\bar{u}k_b}A_a A_b R_a R_b \overline{q_y}\right] = 0 \qquad (8)$$

This equation can be solved only for specific values of the amplitude variations $\partial A_2/\partial t$, because R_2, ω_2, k_2 are solutions of the linear equation (5). Hence a solution exists only if the non-homogeneous part is orthogonal to the homogeneous solution R_2. Now let k_0 correspond to a primary prominent wave and $k_{1,2}$ to secondary waves. After some manipulations we obtain:

$$\frac{\partial A_2}{\partial t}\int_{-\infty}^{\infty}\overline{q_y}R_2^2 dz = A_0 A_1 \frac{(c_1-c_0)(\bar{u}+c_2)}{(\bar{u}+c_1)(\bar{u}+c_0)}(k_0 n_1 - k_1 l_0)\int_{-\infty}^{\infty} R_0 R_1 R_2 \overline{q_y} dz\,, \qquad (9)$$

and replacing of 1 by 2 and 2 by 1 we can get the equation for A_1.

$$\frac{\partial A_2}{\partial t} = \delta_{0,1} A_0 A_1\,,\ \frac{\partial A_1}{\partial t} = \delta_{0,2} A_0 A_2 \qquad (10)$$

The equations (10) are the same as those for internal gravity waves obtained by Davis and Acrivos (1967). From their results it follows that the primary wave is unstable at a condition

$$\delta_{0,1}\,\delta_{02} > 0.$$

We will not proceed this consideration with some possible analytical distributions simply referring to the numerical results. The correct obtaining of equation (3) must take into account a few small parameters: dissipation, non-linearity, ageostrophic terms. And we should determine relations between them.

Conclusions

Basing on numerical calculations we have demonstrated that some changes of the climatological background atmosphere may lead to an unstable mean zonal wind distribution in the summer hemisphere. This instability forces oscillations with period of about 2 day and zonal wavenumbers s = 3 and 4. There are changes in the mean zonal distribution of zonal wind due to the excitation and propagation of these waves and our numerical results correspond to features of these changes obtained in experimental studies.

The strong 2-day waves in turn are unstable and can generate waves with longer periods and lower zonal wavenumbers. This effect is significant only for extremely strong 2-day waves. Another process was found to be more effective in generating secondary waves. During interaction of 10-14 day planetary waves with the 2-day wave of zonal wave number 4 a new 2-day wave is forced with a period of 55-60h, which generates secondary waves of lower zonal wavenumbers more effectively than the primary 2-day wave. These secondary waves may be observed.

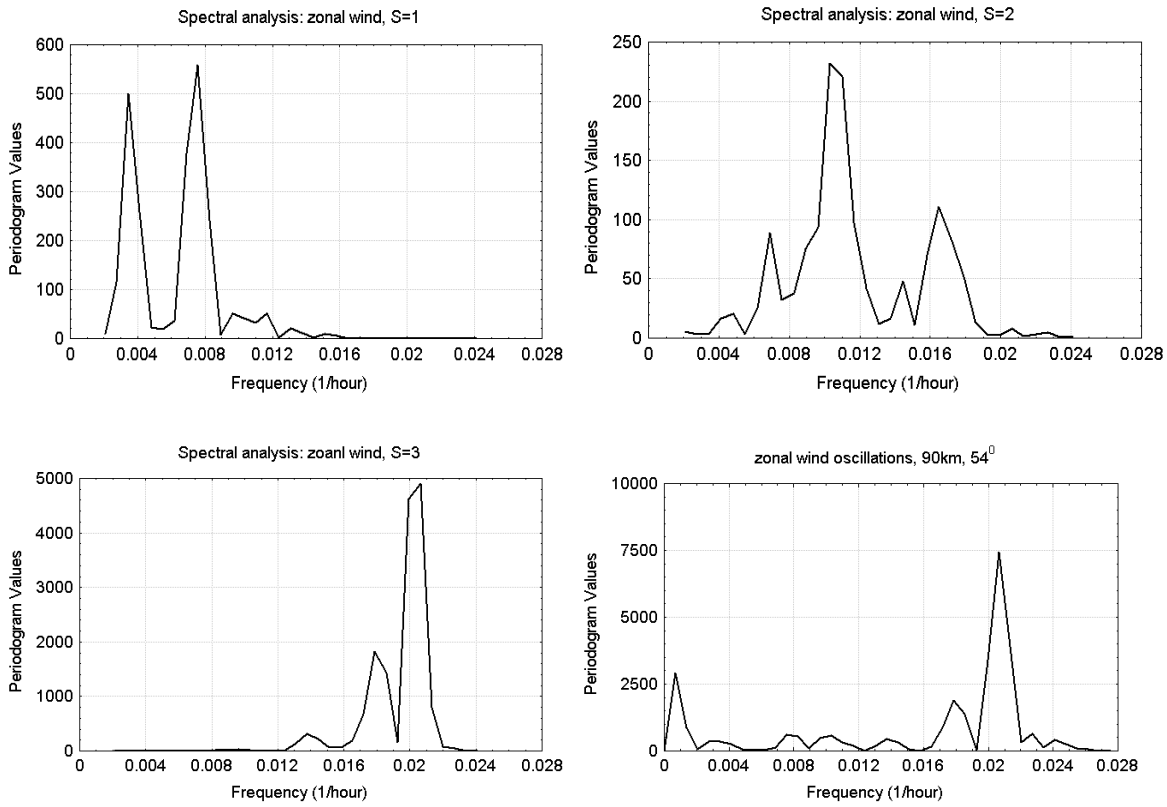

amplitude (m/s) of zonal wind oscillations at 90km, 54^0

longitude 0^0 *longitude 80^0*

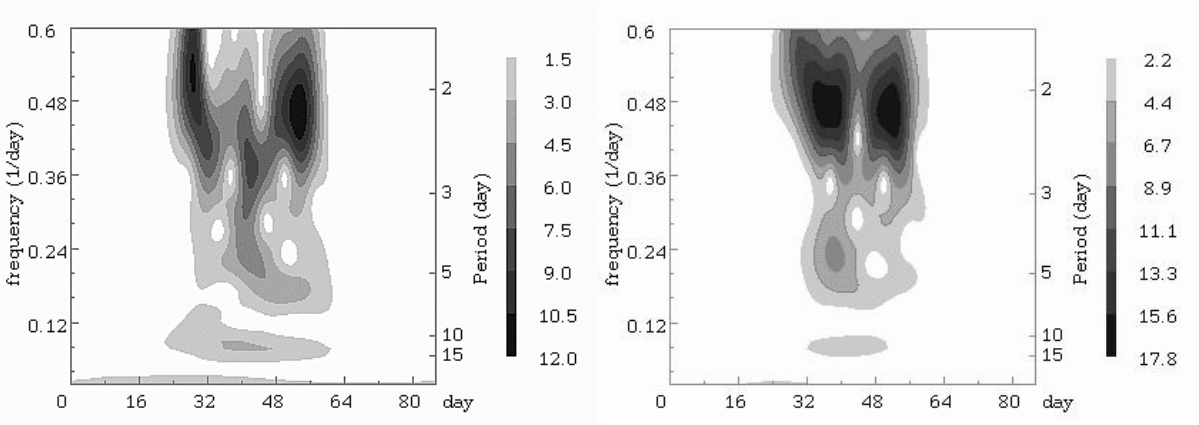

Figure 9: *Interaction between the 2-day wave forced by jet instability and a12-day planetary wave. The results are presented for a 1450-hour run .S-spectra and the relative periodogram are calculated for this time interval at height of 90 km, latitude 54°, and longitude 80°. Amplitudes (m/s) are shown by scale of grey.*

Appendix: Numerical model

The numerical model used for the simulations is based on the one described by Rose (1983) and Jakobs et al. (1986). The horizontal momentum equations, the thermodynamic equation, the continuity equation and the hydrostatic equation in spherical log-pressure co-ordinates are solved by explicit finite-differences. Unlike the model referred to above, we used an expansion in Fourier harmonics in longitude, while instead of a gravity wave parameterisation we

used a body force like that proposed by Fritts and Luo (1995). The radiation processes are parameterised by Newtonian cooling $Q = \alpha (T-T_0)$ where the rate coefficient α was adopted from Zhu (1993) and T_0 is the reference temperature from the CIRA 86 model presented by Fleming et al. (1986). The finite difference grid has a step of $\Delta\varphi = 3°$ in latitude and $\Delta z = 0.25$ in height, where $z=-\ln(P/P_S)$ ranging from $z = 0$ to $z = 22$ and P is the pressure, while $P_S = 1000$ hPa is a reference pressure. The expansion in longitude is performed in terms of $\exp(im\lambda)$, where m (= -6, …+6) is a zonal wavenumber and λ is the longitude.

The coefficients of dynamic molecular viscosity and molecular thermal heat conduction were taken from Forbes and Garrett (1979), eddy viscosity was adopted from Hagan et al. (1995) and hydromagnetic effects are included in a simple form as in Forbes and Gurret (1979). Some horizontal smoothing was applied to calculated fields that is equivalent to horizontal dissipation of fourth order with a rate of about 10^{15} m^4/s. Background field distributions are obtained from a model run with initially motionless atmosphere and horizontally uniform temperature.

At the bottom we imposed the condition $d\Phi/dt = 0$ at z=0, where Φ is the geopotential. For velocity components and the non-zonal component of temperature ($m\neq0$) we used the conditions like those utilised by Forbes (1982) to simulate the influence of the surface. For the mean zonal component of temperature we used a time independent temperature distribution from Fleming et al. (1988).

The log-pressure vertical velocity (dz/dt), vertical gradients of velocities and non-zonal components of temperature ($m\neq0$) are set to 0 at the upper horizontal boundary. The mean zonal component of temperature (m=0) does not depend on time at the upper boundary and was estimated from models of Fleming et al. (1988).

References

Andrews, D.G., J.R. Holton., and C.B. Leovy, Middle Atmosphere Dynamics, 489 pp., Academic, Orlando, Florida, 1987.

Baines, P.G., The stability of planetary waves on a sphere, J. Fluid Mech., 73, 193-213, 1976.

Craig, R.L., L.A. Vincent, G.J. Fraser, and M.J. Smith, The quasi 2-day wave near 90 km altitude at Adelaide (35^0S), Nature, 287, 319-320, 1980.

Davis, R.E. and A. Acrivos, The stability of oscillatory internal waves, J. Fluid Mech., 30, 723-736, 1967.

Fleming, E.L., S. Chandra, M.R. Shoerberl, and J.J. Barnett, Monthly mean global climatology of temperature, wind, geopotential height, and pressure for 0-120 km. NASA Tech. Memorandum, 100697, 85 pp., 1988.

Forbes, J.M., and H.B. Garrett, Theoretical studies of atmospheric tides, Rev. Geophys. Space Phys., 17, 1951-1981, 1979.

Forbes, J.M., Atmospheric tides, 1, Model description and results for the solar diurnal component, J. Geophys. Res., 87, 5222-5240, 1982.

Fritts, D.C., and Z. Luo, Dynamical and radiative forcing of the summer mesopause circulation and thermal structure, I. Mean solstice conditions. Journal of Geophysical Research, 100, 3119-3128, 1995.

Fritts, D.C., J.R. Isler, R.S. Lieberman, M.D. Burrage, D.R. Marsh, T. Nakamura, T. Tsuda, R.A. Vincent, and I.M. Reid, Two-day wave structure and mean flow interactions observed by radar and High resolution Doppler Imager, J. Geophys. Res., 104, 3953-3969, 1999.

Gill, A.E., The stability of planetary waves on an infinite beta-plane, Geophys. Fluid Dyn., 6, 29-47, 1974.

Gurubaran S., S. Sridharan, T.K. Ramkumar, and R. Rajaram, The mesospheric quasi-2-day wave over Tirunelveli (8.7^0N), J. Atmos. Solar-Terr. Phys., 63, 975-985, 2001.

Hagan M.E., J.M. Forbes, and F. Vial, On modeling migrating solar tides, Geophys. Res. Let., 22, 893-896, 1995.

Jacobi, Ch., R. Schminder, and D. Kürschner, The quasi two-day wave as seen from D1 LF wind measurements over Central Europe (52°N, 15°E) at Collm, J. Atmos. Solar-Terr. Phys., 59, 1277-1286, 1997.

Jacobi, Ch., Yu.I. Portnyagin, E.G. Merzlyakov, B.L. Kashcheyev, A.N. Oleynikov, D. Kürschner, N.J. Mitchell, H.R. Middleton, H.G. Muller, V.E. Comley, Mesosphere/lower thermosphere wind measurements over Europe in summer 1998, J. Atmos. Solar-Terr. Phys., 63, 1017-1031, 2001.

Jakobs H.J., M. Bischof, A. Ebel, and P. Speth, Simulation of gravity waves effects under solstice conditions using a 3-D circulation model of the middle atmosphere, J. Atmos. Solar-Terr. Phys., 8, 1203-1223, 1986.

Kal'chenko, B.V., and S.V. Bulgakov, Study of periodic components of wind velocity in the lower thermosphere above the equator, Geomagnetism i Aeronomy, 13, 955-956,1973.

Lieberman, R.S., Eliassen-Palm fluxes of the two-day wave, J. Atmos. Sci., 56, 2846-2861, 1999.

Limpasuvan V., C.B. Leovy, Y.J. Orsolini, Observed temperature two-day wave and its relatives near the stratopause, J. Atmos. Sciences, 57, 1689-1701, 2000.

Mayr H.G., J.G. Mengel, K.L. Chan, and H.S. Porter, Mesosphere dynamics with gravity wave forcing: Part II. Planetary waves, J. Atmos. Solar-Terr. Phys., 63, 1865-1881, 2001.

Muller, H.G., Long-period meteor wind oscillations, Phil. Trans. R. Soc. London, A271, 585-598, 1972.

Pfister L., Baroclinic instability of easterly jets with applications to the summer mesosphere, J. Atmos. Sci., 42, 313-330, 1985.

Plumb R.A., Baroclinic instability of the summer mesosphere: A mechnism for the quasi-two-day wave? J. Atmos. Sci , 40, 262-270, 1983.

Plumb, R.A., R.A. Vincent, and R.L. Craig, The quasi-2-day wave event of January 1984 and its impact on the mean mesospheric circulation, J. Atmos. Sci., 44, 3030-3036, 1987.

Portnyagin, Yu.I., E.G. Merzlyakov, Ch. Jacobi, N.J. Mitchell, H.G. Muller, A.H. Manson, W. Singer, P. Hoffman, and A.N. Fachrutdinova, Some results of S-transform analysis of the transient planetary-scale wind oscillations in the lower thermosphere. Earth, Planets and Space, 51, 711-718, 1999.

Salby, M.L., and P.F. Callaghan, Seasonal amplification of the 2-day wave: relationship between normal mode and instability, J. Atmos. Sci., 58, 1858-1869, 2001.

Stockwell, R.G., L. Mansinha, and R.P. Lowe, Localisation of the complex spectrum: The S transform, IEEE Trans. Signal Proc., 44, 998-1001, 1996.

Wu, D.L., E.F. Fishbein, W.G. Read, and J.W. Waters, Excitation and evolution of the quasi-2-day wave observed in UARS/MLS temperature measurements, J. Atmos. Sci., 53, 728-738, 1996.

Zhu, X., Radiative damping revisited: parameterization of damping rate in the middle atmosphere. J. Atmos. Sci., 50, 3008-3021, 1993.

Addresses of Authors:

E. G. Merzlyakov, Institute for Experimental Meteorology, 82, Lenin Str., Obninsk, Kaluga Reg., 249020, Russland

Ch. Jacobi, Institut für Meteorologie, Universität Leipzig, Stephanstr. 3, 04103 Leipzig, Germany